CrystEngComm

PAPER

Studies on phase stability, mechanical, optical and electronic properties of a new Gd_2CaZnO_5 phosphor system for LEDs†

Cite this: *CrystEngComm*, 2014, **16**, 1652

Dongwei Xu,[a] D. Haranath,*[b] Haiying He,*[c] Savvi Mishra,[b] Isha Bharti,[b] Deepika Yadav,[b] B. Sivaiah,[b] Bhasker Gahtori,[b] N. Vijayan,[b] A. Dhar,[b] Jiajie Zhu,[a] V. Shanker[b] and Ravindra Pandey[a]

Received 28th October 2013,
Accepted 29th November 2013

DOI: 10.1039/c3ce42194e

www.rsc.org/crystengcomm

A new ternary oxide Gd_2CaZnO_5 having interesting structural, mechanical, electronic and optical properties is synthesized and is studied in detail using density functional theory. The analysis revealed two polymorphs: orthorhombic and tetragonal; the orthorhombic phase was found to be the most stable structure under ambient conditions. A high-pressure (hydrostatic) phase transition to the tetragonal phase is predicted at about 4 GPa. This is one of very few reports that depict the phase transition of oxide materials under pressure. The calculated results are in agreement with the X-ray diffraction studies supported by Rietveld analysis. Analysis of the optical properties revealed both polymorphs to be direct-gap semiconductors with low dielectric constants. The calculated elastic constants of both phases satisfy the mechanical stability criteria. It is also identified that the half-filled 4f orbital of Gd induces a strong magnetic spin polarization in the host oxide lattice indicating that the material could be effectively used in versatile applications ranging from biomedical devices to light emitting diodes.

Inorganic luminescent materials (also called "phosphors") have become the subject of renewed research and development due to the requirement of efficient color display systems for next generation lighting and display devices.[1–3] Especially, a family of oxide crystals doped with rare-earth ions have become candidate materials for such display devices due to their highly efficient emission properties which are attributed to the sharp f–f transitions in the visible spectrum.[4] For example, ternary oxides defined by R_2AMO_5 with R = rare-earth, A = alkaline-earth and M = Cu or Zn atoms are found to have the desired luminescent properties for efficient color tunability.[5–10] This family of ternary oxides having large band gaps can serve as good luminescent hosts in accommodating rare-earth ions as dopants and thereby yielding effective luminescence with high quantum efficiency. For instance, the red-emitting Eu^{3+} doped R_2BaZnO_5 is reported to show the quantum efficiency of about 75%.[11,12] Recently, we have synthesized a new red-emitting Gd_2CaZnO_5 phosphor doped with Eu^{3+}, which has a strong absorption in the blue (~465 nm) spectral region.[13] This is significant as the conventional red-emitting Y_2O_3:Eu^{3+} phosphor does not show any absorption for blue (~465 nm) light. Thus, the Eu^{3+}-doped Gd_2CaZnO_5 phosphor could become a replacement for conventional red-emitting phosphors in futuristic white light emitting diodes.

There seems to be a dearth of information about the structural and fundamental properties of the R_2AMO_5 oxides, though their luminescence properties have been well characterized.[13] A relationship between the lattice structure and the nature of the constituent atoms forming the lattice has yet to be established. In other words, R_2BaZnO_5 can crystallize in either orthorhombic or tetragonal phases under ambient conditions depending on the nature of the cations; Dy_2SrCuO_5 is orthorhombic with a space group of *Pnma*, (no. 62)[14] and Nd_2BaZnO_5 is tetragonal with a space group of *I*4/*mcm* (no. 140).[15] This has prompted us to undertake a detailed investigation of the physical and chemical properties of the Gd_2CaZnO_5 phosphor system‡ using first-principles methods based on density functional theory (DFT).[16,17] The photoluminescence excitation and emission characteristics of the

[a] *Department of Physics, Michigan Technological University, Houghton, Michigan 49931, USA*
[b] *CSIR-National Physical Laboratory, Dr. K. S. Krishnan Road, New Delhi, 110 012, India. E-mail: haranath@nplindia.org; Fax: +91 11 4560 9310*
[c] *Department of Physics and Astronomy, Valparaiso University, Valparaiso, Indiana 46383, USA*

† Electronic supplementary information (ESI) available: Photoluminescence studies and flow chart depicting the synthesis of Gd_2CaZnO_5 phosphor. See DOI: 10.1039/c3ce42194e

Gd_2CaZnO_5 phosphor have been studied in detail and are shown in Fig. S1 (see ESI†). The broad yellow emission at ~560 nm is very suitable as an alternative phosphor in white light emitting devices. In particular, we will determine the phase stability, mechanical, electronic and optical properties of the Gd_2CaZnO_5 lattice system. Ca and Ba being alkaline-earth elements, the physical properties are expected to be similar for Gd_2CaZnO_5 and Gd_2BaZnO_5 material systems. Furthermore, it is highly expected that the physics involved in these oxide materials is likely to be governed by the basic structure motif of Gd_2O_{11} in the lattice.

Computational method

The projector augmented plane-wave (PAW) method as implemented in the Vienna *ab initio* simulation package (VASP) is employed to calculate the electronic structure of the Gd_2CaZnO_5 crystal.[18,19] The generalized gradient approximation (GGA) of Perdew, Burke and Ernzerhof (PBE) is adopted for the exchange–correlation potential[20] to density functional theory (DFT). The $4f^7 5d^1 6s^2$ electrons of Gd are considered as the valence electrons in the calculations, and an additional Hubbard term, *U*, is employed to represent the on-site Coulomb interactions for the localized 4f orbitals. The relative value of the $U - J$ parameter is set to 7 eV, which was previously used to investigate the Gd pnictides.[21] The *k*-points chosen for the Brillouin-zone integrations are 4 × 6 × 6 and 6 × 6 × 4 for the orthorhombic and tetragonal crystalline conventional cells, respectively. The cut-off energy for the plane-wave basis set has been taken as 370 eV. The energy tolerance is 10^{-6} eV in the iterative solution of the Kohn–Sham equations. The structure and atoms are relaxed until the force on each atom is less than 0.01 eV $Å^{-1}$. It has been observed that the chosen *k*-point mesh, cut-off energy and tolerance parameters yield convergence of the total energies to be ~5 meV per formula unit for the ternary oxide systems.

The elastic constants are determined using second-order derivatives of equilibrium energy with respect to strains *via* the equation:

$$C_{\alpha\beta} = \frac{1}{V}\frac{\partial^2 E}{\partial\gamma_\alpha \partial\gamma_\beta}, \tag{1}$$

where, γ is the applied strain in Voigt's notion around the equilibrium position.[22]

The refractive index has been calculated using the equation:

$$n(\omega) = \left(\frac{\sqrt{{\varepsilon_1}^2(\omega) + {\varepsilon_2}^2(\omega)} + \varepsilon_1(\omega)}{2} \right)^{1/2} \tag{2}$$

The imaginary part of the dielectric function, $\varepsilon_2(\omega)$, is determined by summation over empty states using the equation:

$$\varepsilon_2^{\alpha\beta}(\omega) = \frac{4\pi^2 e^2}{V} \lim_{q\to 0} \frac{1}{q^2} \sum_{c,v,k} 2\omega_k \delta(\epsilon_{ck} - \epsilon_{vk} - \omega) \times \left\langle u_{ck+e_\alpha q} \middle| u_{vk} \right\rangle \left\langle u_{ck+e_\beta q} \middle| u_{vk} \right\rangle^* \tag{3}$$

where the indices *v* and *c* refer to the valence band and conduction band, respectively, and u_{ck} is the cell periodic part of the wave function at different *k*-points.[23]The real part of the dielectric function has been obtained from the Kramers–Kronig transformation using the equation:

$$\varepsilon_1(\omega) = 1 + \frac{2}{\pi}\int_0^\infty \frac{\omega' \varepsilon_2(\omega')\mathrm{d}\omega'}{\left(\omega'^2 - \omega^2\right)} \tag{4}$$

Results and discussion

Structural properties

In order to find the ground state of Gd_2CaZnO_5 under the ambient conditions, we have performed calculations on both orthorhombic and tetragonal phases for which the representative polyhedral structures are shown in Fig. 1. The choice of the orthorhombic or tetragonal phases follows from the established guidelines for the R_2AMO_5 oxide system with R = rare-earths, A = Ba and M = Co, Ni, Cu, Zn, Pd, Pt.[24]

The basic structural units of orthorhombic Gd_2CaZnO_5 consist of the GdO_7, CaO_{11} and ZnO_5 polyhedral units. This orthorhombic structure exhibits similar environments of Gd and Zn ions in the crystal as reported by Wong-Ng *et al.*[14] for R and Cu in R_2SrCuO_5. The Gd atoms occupy two types of non-equivalent positions in the lattice. Each Gd atom is seven-fold coordinated by a monocapped trigonal prism of oxygen atoms. Two such prisms with slightly different Gd–O

‡ Preparation of *GCZO nanophosphor*: a modified citrate-gel combustion method has been employed to prepare the Gd_2CaZnO_5 phosphor system. The gadolinium oxide is dissolved in a stoichiometric amount of concentrated nitric acid to make $Gd(NO_3)_3$. The required metal nitrates of calcium and zinc are added to the solution. All these precursor solutions are mixed together and rigorously stirred with citric acid (metal to citric acid is in 1 : 4 molar ratio) dissolved in water for 15 minutes. The overall pH of the solution is maintained at around 1–2 in order to control the shape and size of the phosphor particles. Citric acid acts as the monomer to form a transparent complex gel from the initial solution upon drying overnight in an oven at 75 °C. Furthermore, the gel is taken in a quartz boat and is fired in air in a pre-heated furnace at 800 °C for 15 minutes. Initially, the citrate complex gel transforms to a black fluffy mass nearly ten times the gel volume and starts to decompose into CO_2 and H_2O vapors in the furnace. After 15 minutes, a white fluffy mass of Gd_2CaZnO_5 is obtained which could easily be crushed to an ultra-fine phosphor. It is then consolidated using a hydraulic press at 10 000 psi and is annealed in a muffle furnace at 1275 °C for 48 hours that resulted in a high density (~3500 kg m^{-3}) solid mass of Gd_2CaZnO_5. Synthesis of high quality material with considerable yield (~90%) is one of the highlights of the proposed method. A flow chart depicting the step-by-step process of synthesizing Gd_2CaZnO_5 phosphor is shown in Fig. S2 (see ESI†).Characterization: the X-ray diffraction (XRD) pattern of the polycrystalline Gd_2CaZnO_5 is obtained using the D8 Advance X-ray diffractometer (Bruker make; Source: $CuK\alpha_1$) at a scan speed of 1° min^{-1} at room temperature. The Miller indices (*h k l*) and lattice parameters are determined using the standard WIN-INDEX (ver. 3.08) software package and are refined by Rietveld analysis using the Fullprof software. All the observed reflections were indexed with the least square fit method. The elastic properties have been measured at room temperature (305 K) using the nanoindentation technique at a load of 50 mN.

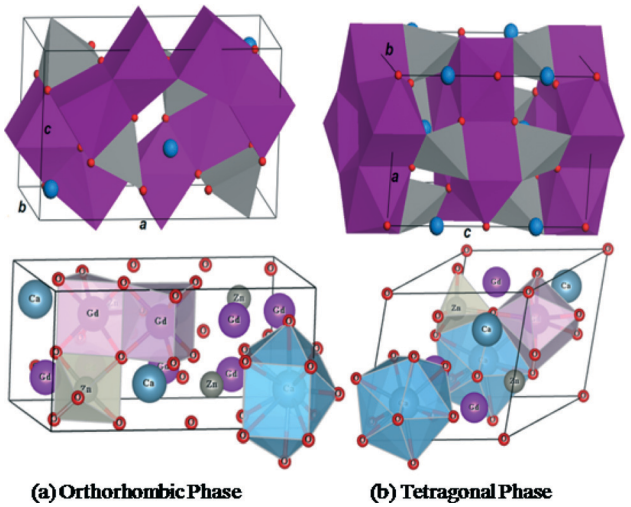

Fig. 1 Gd_2CaZnO_5 (a) orthorhombic and (b) tetragonal phases. Polyhedron representation of the structures are shown in the upper panel (conventional cells), while only representative bonds for each type of polyhedral structure unit are shown for clarity in the lower panel (primitive cells) (red: oxygen, purple: gadolinium; grey: zinc; dark cyan: calcium) (colored figure online).

distances share faces or edges to form chains parallel to the diagonal of *a*- and *c*-axes forming a basic structure motif of Gd_2O_{11}. The 5-fold coordinated square pyramids of ZnO_5 are also shown in Fig. 1(a). The Ca–O contact distances cover a broad range of values. A total of seven Ca–O distances have been observed between 2.35 and 2.95 Å, while the remaining four Ca–O distances are between 3.68 and 3.80 Å.

For the tetragonal phase of Gd_2CaZnO_5, the conventional cell contains two primitive cells (Fig. 1(b)). It consists of a three-dimensional array of face- and edge-sharing CaO_{10} and GdO_8 polyhedra. The CaO_{10} coordination polyhedron is a twisted square prism capped on both ends by tetragonal pyramids with the O atoms situated at the corners of the twisted cubic structure and the other O atoms at the top of the caps. The Ca–O distances are nearly equal to 2.83 Å. The GdO_8 polyhedron is a trigonal prism capped on two of the three rectangular faces. They form a condensed layer along the *ab*-plane *via* face-sharing between the adjacent GdO_8 units (Fig. 1(b)). The Zn atoms have tetrahedral coordination with the ZnO_4 groups alternating with the Ca polyhedra in the *ab*-plane.

The calculated DFT values of lattice constants, internal coordinates and cohesive energies of the polymorphs of Gd_2CaZnO_5 are listed in Table 1 together with the measured structural parameters.

The calculated cohesive energy per formula unit suggests that the most stable phase of Gd_2CaZnO_5 is orthorhombic under ambient conditions (Table 1). Note that the cohesive energy is defined as the difference between the energy of Gd_2CaZnO_5 and the sum of total energies of the constituent atoms. For the orthorhombic Gd_2CaZnO_5 with four formula units per unit cell, the DFT results of the lattice parameters are as follows: a = 12.286 Å, b = 5.752 Å and c = 7.219 Å. For the tetragonal Gd_2CaZnO_5 with two formula units per unit cell, the calculated lattice parameters are found to be: a = 6.557 Å and c = 11.323 Å.

The X-ray diffraction measurements are carried out to determine the structure of the synthesized Gd_2CaZnO_5 phosphor, and Rietveld refinement of the sample is carried out at room temperature (~20 °C). The peak corresponding to the (1 2 $\bar{1}$) plane has the maximum intensity counts (Fig. 2).

We find the phosphor to crystallize in an orthorhombic structure (space group = *Pnma*) with the lattice constants: a = 12.453 Å, b = 5.556 Å, c = 7.287 Å and $\alpha = \beta = \gamma = 90°$. The measured values of lattice constants and internal coordinates compare fairly well with the DFT results (Table 1). The other Rietveld refined parameters obtained are R_p = 21.3, R_{wp} = 28.6, R_{exp} = 17.39, χ^2 = 3. Apart from Gd_2CaZnO_5, minor peaks related to ZnO are also observed (marked by * in Fig. 2(b)).

Considering the difference in the cohesive energy of the orthorhombic and tetragonal phases to be small (≈0.14 eV), the possibility of a high-pressure phase transition from the orthorhombic to the tetragonal phase of Gd_2CaZnO_5 is also investigated. The total energy per formula unit is plotted as a function of the unit cell volume of the two polymorphs, and is shown in Fig. 3.

Table 1 The calculated (DFT) and measured (XRD) structural properties of Gd_2CaZnO_5

	Orthorhombic (Rietveld refined)	Orthorhombic (calculated)	Tetragonal (calculated)
Space group	*Pnma*	*Pnma*	*I4/mcm*
Cohesive energy (eV)	—	−80.81	−80.67
Unit cell volume (Å^3)	504.19	510.16	486.36
Lattice constants			
a (Å)	12.453	12.286	6.556
b (Å)	5.556	5.752	6.556
c (Å)	7.287	7.219	11.313
Fractional coordinates			
Ca	0.9233 0.9004 0.2500	0.9329 0.8671 0.2500	0.0000 0.0000 0.2500
Zn	0.6942 0.6505 0.2500	0.6999 0.6618 0.2500	0.0000 0.5000 0.2500
Gd_I	0.1220 0.2937 0.2500	0.1206 0.2897 0.2500	0.1730 0.6730 0.0000
Gd_{II}	0.3956 0.2500 0.0000	0.3930 0.2500 0.0724	
O_I	0.1670 0.4370 −0.0130	0.1670 0.4347 0.0106	0.0000 0.0000 0.0000
O_{II}	0.3550 0.2430 0.4800	0.3335 0.2109 0.4860	0.8472 0.3472 0.6335
O_{III}	0.0750 0.1060 0.2500	0.0530 0.0904 0.2500	

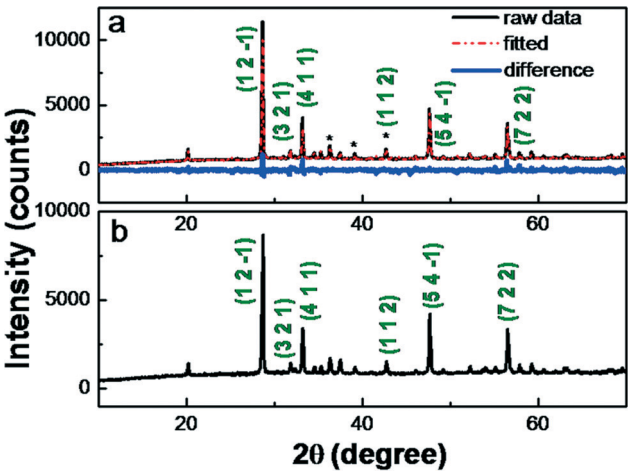

Fig. 2 (a) The X-ray diffraction profile of Gd_2CaZnO_5 recorded at ~20 °C. (b) The (*h k l*) values determined using the standard WIN-INDEX (ver. 3.08) software are shown and have been refined by Rietveld refinement using the Fullprof software. (Colored figure online).

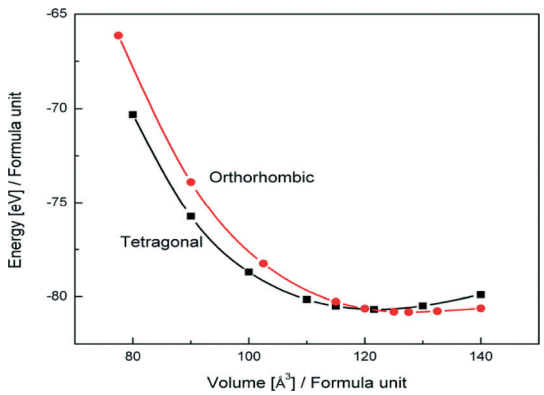

Fig. 3 Total energy per formula unit as a function of unit cell volume for Gd_2CaZnO_5. (Colored figure online).

The lattice parameters as well as the internal coordinates have been optimized at each fixed value of unit-cell volume for both phases. It is known that the high-pressure phase transition would be at the pressure where the enthalpy defined by $H = E + PV$ of two phases is equal. A close examination of such a plot (Fig. 4) suggests the transition pressure to be at about 4.1 GPa for Gd_2CaZnO_5. At zero pressure, the equilibrium unit cell volume of the tetragonal phase relative to that of the orthorhombic phase turns out to be 0.95 (Table 1). Therefore, it could be concluded that the orthorhombic phase would be much stable under ambient conditions as also evidenced experimentally.

Elastic properties

The calculated elastic properties, including elastic constants, bulk and shear moduli and Debye temperature of the polymorphs of Gd_2CaZnO_5 are shown in Table 2. In addition to that, we have measured some of the elastic properties using the nanoindentation technique which are indicated in Table 2.

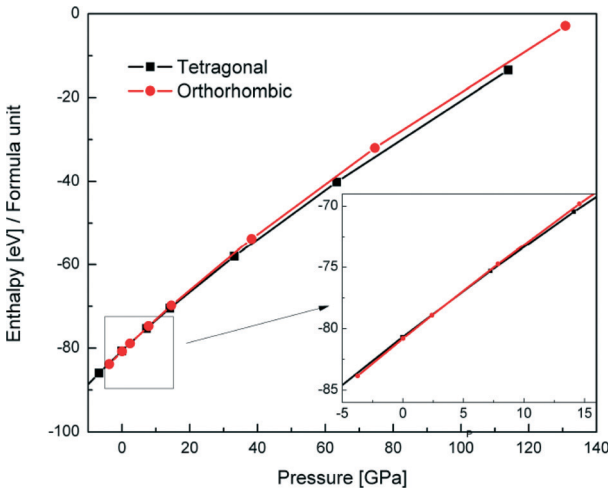

Fig. 4 Enthalpy pressure curve for polymorphs of Gd_2CaZnO_5. Inset shows the enlarged view of a specific area. (Colored figure online).

Table 2 The calculated and measured elastic properties of Gd_2CaZnO_5

	Orthorhombic (calculated/measured)	Tetragonal (calculated/measured)
Elastic constant (GPa)		
C_{11}	232.1/218	193.1/199
C_{12}	73.2	77.0
C_{13}	90.0	65.9
C_{22}	226.3	
C_{23}	52.9	
C_{33}	147.0	211.5
C_{44}	23.1	18.3
C_{55}	74.7	
C_{66}	38.3	70.0
Bulk modulus (GPa)		
K_V	115.3	112.8
K_R	108.9	112.8
K_H	112.1	112.8
Shear modulus (GPa)		
G_V	53.2	47.2
G_R	42.8	32.3
G_H	48.0	39.8
Directional Young modulus (GPa)		
B_X	169.0/160.0	154.1/155.2
B_Y	197.9	
B_Z	109.1	179.4
Debye temperature (K)	373.6/305	338.7/305

The elastic constants of the orthorhombic structure have been characterized by nine independent components, *i.e.* C_{11}, C_{12}, C_{13}, C_{22}, C_{23}, C_{33}, C_{44}, C_{55} and C_{66}. In the case of the tetragonal phase, the independent components would reduce to six. For both orthorhombic and tetragonal phases, the calculated elastic constants satisfy the mechanical stability criteria,[25,26] thereby suggesting that both are mechanically stable.

K and G are average bulk and shear moduli, respectively. The subscripts V, R and H have been used to denote the Voigt, Reuss and Hill notations, respectively, where K_H (G_H) is the average value of K_V (G_V) and K_R (G_R). The calculated

values of bulk modulus are comparable for the two phases, while the value of shear modulus for the orthorhombic phase is consistently higher than that for the tetragonal phase for different notations. This could be due to the alternating layered structure of the tetragonal phase. B_X is the bulk modulus along the x-axis of a system under hydrostatic pressure. As the dispersion in the directional bulk moduli along different crystal axes reveals the anisotropy of the system, the percentage of anisotropy could be calculated as $((B_X - B_Z)/(B_X + B_Z) \times 100\%)$ for both the x and z directions in the lattice. It is to be noted that the envisaged anisotropy is ~7.6% along x and z directions for the tetragonal phase and for the orthorhombic phase, it is ~21.5%. A larger anisotropy in the orthorhombic structure might arise from the distorted chains formed by the two GdO_7 trigonal prisms in Gd_2CaZnO_5. No experimental evidence is available for comparison with the envisaged anisotropy values.

Electronic properties

The calculated band structures of Gd_2CaZnO_5 have been shown in Fig. 5 for spin-up and spin-down electrons. In general, the band structures of these two phases are very similar (Table 3). The anionic and cationic states constitute the top of the valence and the bottom of the conduction band, respectively.

Note that the k-points are Γ = (0, 0, 0), Z = (0, 0, 1/2), T = (−1/2, 0, 1/2), Y = (−1/2, 0, 0), S = (−1/2, 1/2, 0), X = (0,1/2, 0), U = (0, 1/2, 1/2) and R = (−1/2, 1/2, 1/2) for the orthorhombic phase. For the tetragonal phase, the k-points are Z = (1/2, 1/2, −1/2), Γ = (0, 0, 0), X = (0, 0, 1/2), P = (1/4, 1/4, 1/4) and N = (0, 1/2, 0). Both phases have direct band gaps. In addition, the spin-up and spin-down electron bands share a lot of similarity (comparing Fig. 5(a1) with (a2); Fig. 5(b1) with (b2)). The distinct difference comes from the Gd 4f bands, which are 6.48 eV (orthorhombic) and 6.12 eV (tetragonal) below the top of valence band for the spin-up electrons, and 5.96 eV (orthorhombic) and 6.27 eV (tetragonal) above the top of valence band for the spin-down electrons. The (minimum) energy gap is 2.61 (spin-up)/2.74 (spin-down) and 3.22 (spin-up)/2.49 (spin-down) eV at Γ or Z for the orthorhombic and tetragonal phases, respectively. It should be pointed out that the GGA-DFT level of theory underestimates the band gap of oxides. Nevertheless, distinct features in the band structures of the Gd_2CaZnO_5 polymorphs have been clearly demonstrated by the method employed in the current study.[27]

As shown in Fig. 6, the O 2p orbitals dominate the upper valence band, while the Zn 3d orbitals lie at −5.01 eV below the top of the valence band for both phases. The lower conduction band is dominated by states associated with Ca. The contributions from spin-up electrons are almost degenerate with the spin-down electrons, except for the Gd 4f orbitals, whose spin-up orbitals lie deeper at −6.48 and −6.12 eV below the top of the valence band for the orthorhombic and tetragonal phases, respectively. These Gd 4f orbitals are half-filled leading to the magnetic moment of 14 μ_B in the ground state of Gd_2CaZnO_5.[28]

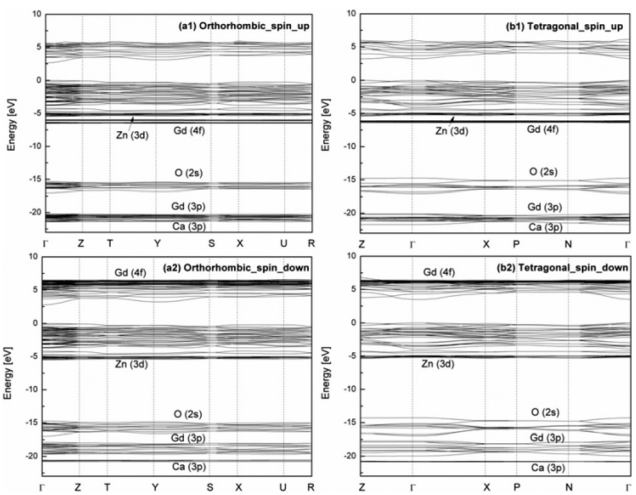

Fig. 5 Band structures of Gd_2CaZnO_5 in (a) orthorhombic and (b) tetragonal phases. Zero of energy is aligned to the top of the valence band.

Optical properties

Fig. 7 depicts the dielectric function of Gd_2CaZnO_5 in orthorhombic and tetragonal phases. Their similarity is a direct reflection of the similarity in their band structures shown in Fig. 5. Theoretical studies offer the advantage of identifying the transitions that are responsible for the peaks in ε_2 using the calculated band structures.[29] It will assist researchers in

Table 3 Electronic and optical properties of Gd_2CaZnO_5

		Orthorhombic		Tetragonal	
		Spin-up	Spin-down	Spin-up	Spin-down
Direct band gap (eV)	Γ	2.61	2.74	—	2.49
	Z	—	—	3.22	—
Location of bands with respect to top of the valence band (eV)	Zn (3d)	−5.01	−5.01	−5.03	−5.03
	Gd (4f)	−6.48	−5.96	−6.12	−6.27
	O (2s)	−15.99	−15.62	−15.14	−15.04
	Ca (3p)	−20.56	−20.56	−20.87	−20.87
Valence band width (eV)		3.66	3.48	3.64	3.64
Static dielectric constant		6.19		4.72	
Refractive index		2.49		2.17	

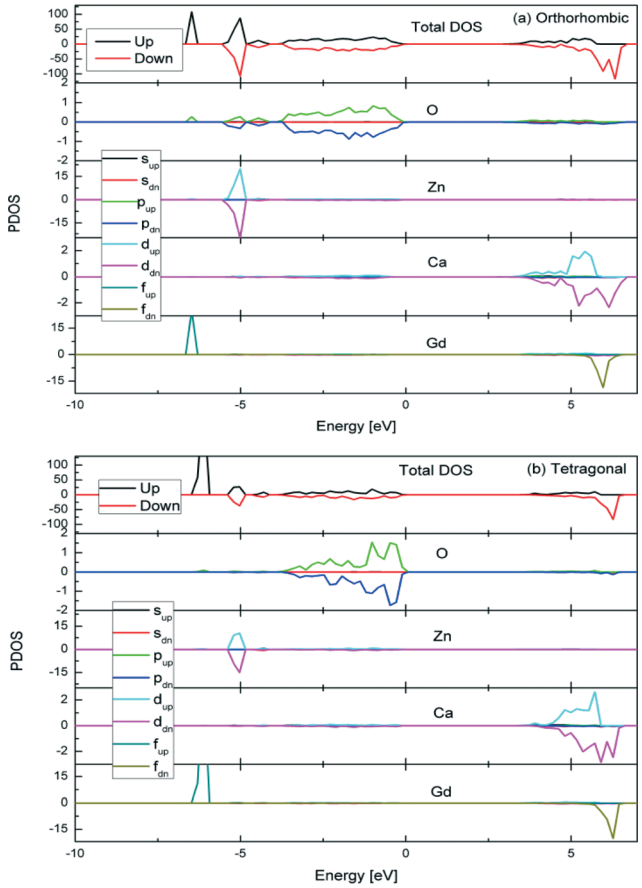

Fig. 6 Projected density of states of Gd_2CaZnO_5 in orthorhombic and tetragonal phases. Zero of energy is aligned to top of the valence band. (Colored figure online).

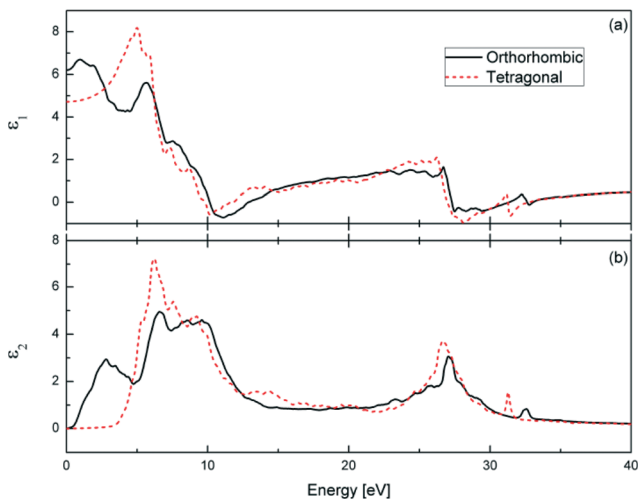

Fig. 7 Calculated (a) real part ε_1 and (b) imaginary part ε_2 of dielectric function of polymorphs of Gd_2CaZnO_5. (Color figure online).

identifying the peaks in the optical spectra obtained by either reflectance or photoelectron spectroscopy.

The major band located around 7 eV is attributed to the inter-band transitions from the Zn 3d valence band to the conduction band associated with Ca. This band has more pronounced peaks in the tetragonal phase of Gd_2CaZnO_5 due to its higher degeneracy. The smaller peak at about 27 eV originates from the excitation of electrons associated with Ca from valence to conduction levels in the lattice.

The calculated values of the dielectric constants ε are listed in Table 3, together with the refractive indices $n = \sqrt{\varepsilon}$ for both orthorhombic and tetragonal phases of the Gd_2CaZnO_5 polymorphs at zero pressure. The dielectric function can be used to describe the linear response of the system to electromagnetic radiation, which is related to the interaction of photons with electrons. Note that ε is obtained from the zero-frequency limit of ε_1, and it corresponds to the electronic part of the static dielectric constant of the material, a parameter of fundamental importance in many aspects of material properties. For the orthorhombic phase, the calculated dielectric constant is 6.19 while it is 4.72 for the tetragonal phase. It is known that the dielectric constant is directly related to the polarizability of the crystal. The polarizability, which represents the deformability of the electronic distribution, is connected with the shape of the valence charge density. A larger dielectric constant of Gd_2CaZnO_5 in the orthorhombic phase can be attributed to the denser packing of ions (*i.e.* distorted chains formed by the two GdO_7 trigonal prisms) relative to the tetragonal phase.

Conclusions

The results pertaining to the synthesis and various physical properties of Gd_2CaZnO_5 polymorphs are reported. The detailed first-principles analysis of polyhedral structures revealed two polymorphs namely orthorhombic and tetragonal phases. The orthorhombic phase has been found to be the most stable phase confirmed by the experimental measurements, though the phase transition to the tetragonal phase does not require a very high pressure. The optical properties of the orthorhombic and tetragonal phases revealed that both polymorphs are direct-gap semiconductors with low dielectric constants. Out of these, the orthorhombic phase exhibits a lower band-gap and higher dielectric constant as compared to the tetragonal phase. It is also identified that the half-filled 4f orbital of Gd induces a strong magnetic spin polarization in the host oxide lattice. Being a direct band-gap semiconducting material with interesting properties, Gd_2CaZnO_5 is a candidate material for efficient color display systems for the next generation communication and entertainment devices.

Acknowledgements

The authors (DH and SM) gratefully acknowledge the Department of Science and Technology, Government of India for the financial support under the scheme # SR/FTP/PS-012/2010 to carry out the above research work. We thank S. Gowtham for his helpful discussion and suggestions.

Notes and references

1 H. Yamamoto and S. Okamoto, *Displays*, 2000, **21**, 93.
2 C. H. Kim, I. E. Kwon, C. H. Park, Y. J. Hwang, H. S. Bae, B. Y. Yu, C. H. Pyun and G. Y. Hong, *J. Alloys Compd.*, 2000, **311**, 33.
3 L. Yi, Y. Hou, H. Zhao, D. He, Z. Xu, Y. Wang and X. Xu, *Displays*, 2000, **21**, 147.
4 C. Feldmann, T. Justel, C. R. Ronda and P. J. Schmidt, *Adv. Funct. Mater.*, 2003, **13**, 511.
5 I. Etchart, A. Huignard, M. Berard, M. N. Nordin, I. Hernandez, R. J. Curry, W. P. Gillind and A. K. Cheetham, *J. Mater. Chem.*, 2010, **20**, 3989.
6 C.-H. Liang, Y.-C. Chang and Y.-S. Chang, *Appl. Phys. Lett.*, 2008, **93**, 211902.
7 C. Michel, L. Er-Rakho and B. Raveau, *J. Solid State Chem.*, 1982, **42**, 176.
8 C. Michel and B. Raveau, *J. Solid State Chem.*, 1982, **43**, 73.
9 C. Michel and B. Raveau, *J. Solid State Chem.*, 1983, **49**, 150.
10 G. K. Cruz, H. C. Basso, M. C. Terrile and R. A. Carvalho, *J. Lumin.*, 2000, **86**, 155.
11 M. J. Lammers, H. Donker and G. Blasse, *Mater. Chem. Phys.*, 1985, **13**, 527.
12 A. Hernandez-Perez, E. Camarillo, M. E. Villafuerte-Castrejon, L. Bucio, M. C. Flores, J. Hernandez and H. Murrieta, *Opt. Mater.*, 2006, **28**, 336.
13 S. Mishra, R. Rajeswari, N. Vijayan, V. Shanker, M. K. Dalai, C. K. Jayasankar, S. Surendra Babu and D. Haranath, *J. Mater. Chem. C*, 2013, **1**, 5849.
14 W. Wong-Ng, T. Haugan, J. A. Kaduk, R. A. Young, Z. Yang, M. H. Jang and M. Luong, *J. Solid State Chem.*, 2006, **179**, 1588.
15 H. C. Gupta and V. Sharma, *J. Raman Spectrosc.*, 2007, **38**, 1554.
16 V. I. Anisimov, F. Aryasetiawan and A. I. Lichtenstein, *J. Phys.: Condens. Matter*, 1997, **9**, 767.
17 R. G. Parr, *Annu. Rev. Phys. Chem.*, 1983, **34**, 631.
18 G. Kresse and J. Furthmüller, *Phys. Rev. B: Condens. Matter Mater. Phys.*, 1996, **54**, 11169.
19 G. Kresse and D. Joubert, *Phys. Rev. B: Condens. Matter Mater. Phys.*, 1999, **59**, 1758.
20 J. P. Perdew, K. Burke and M. Ernzerhof, *Phys. Rev. Lett.*, 1996, **77**, 3865.
21 S. Abdelouahed and M. Alouani, *Phys. Rev. B: Condens. Matter Mater. Phys.*, 2007, **76**, 214409.
22 D. Groh, W. J. Slough, R. Pandey, S. P. Karna and D. Dandekar, *Phys. Rev. B: Condens. Matter Mater. Phys.*, 2011, **83**, 115122.
23 M. Gajdoš, K. Hummer, G. Kresse, J. Furthmüller and F. Bechstedt, *Phys. Rev. B: Condens. Matter Mater. Phys.*, 2006, **73**, 045112.
24 J. K. Burdett and J. F. Mitchell, *J. Am. Chem. Soc.*, 1990, **112**, 657.
25 D. C. Wallace, *Thermodynamics of Crystals*, Wiley, New York, 1972, ch. 1.
26 O. Beckstein, J. E. Klepeis, G. L. W. Hart and O. Pankratov, *Phys. Rev. B: Condens. Matter Mater. Phys.*, 2001, **63**, 134112.
27 B. I. Min and Y. R. Jang, *J. Phys.: Condens. Matter*, 1991, **3**, 5131.
28 A. B. Shick, W. E. Pickett and C. S. Fadley, *Phys. Rev. B: Condens. Matter Mater. Phys.*, 2000, **61**(14), 9213.
29 S. Baroni and R. Resta, *Phys. Rev. B: Condens. Matter Mater. Phys.*, 1986, **33**, 7017.